

## Article

# Mechanistic Insights into the Anticancer Activity of the Crotalicidin-Derived Ctn-2 Peptide in Triple-Negative Breast Cancer

Ana María Sepúlveda <sup>1</sup>, Marcela Manrique-Moreno <sup>2</sup>, Sofía Echeverri-Gaviria <sup>2</sup> and Gloria A. Santa-González <sup>1,3,\*</sup>

<sup>1</sup> Grupo de Investigación e Innovación Biomédica GI2B, Facultad de Ciencias Exactas y Aplicadas, Instituto Tecnológico Metropolitano, Medellín 050034, Colombia; anasepulveda189417@correo.itm.edu.co

<sup>2</sup> Chemistry Institute, Faculty of Exact and Natural Sciences, University of Antioquia-UdeA, A.A 1226, Medellín 050010, Colombia; marcela.manrique@udea.edu.co (M.M.-M.); sofia.echeverri@udea.edu.co (S.E.-G.)

<sup>3</sup> Grupo de Investigación en Biología Médica BioMed, Facultad de Ciencias Exactas y Aplicadas, Instituto Tecnológico Metropolitano, Medellín 050034, Colombia

\* Correspondence: gloriasanta@itm.edu.co

## Abstract

Triple-negative breast cancer is the subtype with the worst prognosis and has limited treatment options. Bioactive peptides are a promising alternative, having demonstrated antitumor properties with a mechanism of action involving the cell membrane. In this study, we evaluated the Ctn-2 peptide, a fragment of crotalicidin (Ctn), which has shown antitumor activity with highly lytic characteristics but is not selective in non-tumor cells. We evaluated the antitumor activity of the peptide Ctn-2 in triple-negative breast cancer cells and its selectivity over non-tumoral cells. Comparative analyses with LTX-315 and biophysical studies on model membranes indicate that Ctn-2 preferentially interacts with cancer-associated lipids. Functional assays further show that its action involves controlled membrane disruption and associated cellular responses. We also examined the combined effect of Ctn-2 and doxorubicin, finding that Ctn-2 selectively enhanced cytotoxicity in tumor cells and potentiated the activity of conventional chemotherapy. Overall, the results indicate that Ctn-2 is a membrane-active peptide with selective antitumor potential and the ability to improve chemotherapeutic efficacy.

**Keywords:** bioactive peptides; triple negative breast cancer; anticancer peptides; membrane disruption



Academic Editor: Valentina Onnis

Received: 13 December 2025

Revised: 21 January 2026

Accepted: 1 February 2026

Published: 14 February 2026

**Copyright:** © 2026 by the authors.

Published by MDPI on behalf of the Österreichische Pharmazeutische Gesellschaft. Licensee MDPI, Basel, Switzerland. This article is an open access article distributed under the terms and conditions of the [Creative Commons Attribution \(CC BY\) license](https://creativecommons.org/licenses/by/4.0/).

## 1. Introduction

Breast cancer (BC) remains the most frequently diagnosed malignancy worldwide and the leading cause of cancer-related mortality among women. Although predominantly a female disease, it also occurs in men, accounting for approximately 1% of all cases. In 2022 alone, the International Agency for Research on Cancer (IARC), reported nearly 670,000 deaths attributable to BC, underscoring the persistent and growing global health burden it poses [1]. This number continues to increase every year, demonstrating the serious health crisis represented by BC. Among its clinical subtypes, triple-negative breast cancer (TNBC) is of the most therapeutically challenging forms. Defined by the absence of estrogen, progesterone, and HER2 receptors, TNBC lacks actionable molecular targets, which not only limits treatment options but also contributes to its aggressive biological behavior [2]. TNBC comprises 15–20% of all BC diagnoses and disproportionately affects

younger women under 40 years of age. Its high proliferative index, rapid progression, and propensity for early metastasis result in poor clinical outcomes, including a heightened risk of early relapse and significantly reduced survival [3].

Current management of TNBC relies primarily on surgery, radiotherapy, and systemic chemotherapy. However, these approaches are constrained by substantial toxicity, limited long-term efficacy, and the frequent emergence of chemoresistance, all of which profoundly diminish patients' quality of life [3]. This therapeutic gap has intensified the search for novel agents capable of selectively targeting TNBC while minimizing adverse effects. In this context, bioactive peptides (BAPs) have gained increasing attention due to their cationic and amphipathic nature, preferential interaction with negatively charged cancer cell membranes, and mechanisms that often involve direct disruption of membrane integrity. Originally characterized as antimicrobial agents, these peptides have since been categorized into antimicrobial/anticancer peptides, with the latter demonstrating reduced susceptibility to conventional resistance mechanisms and promising activity against a variety of tumor models [4,5]. Snake venoms represent an abundant source of such bioactive molecules, containing proteins and peptides with well-documented antimicrobial and antitumor properties [6]. Crotalicidin, a peptide derived from the American rattlesnake, was initially identified for its antimicrobial activity but has subsequently shown potent antitumor effects in several cancer systems [7,8]. Nevertheless, its cytotoxicity toward healthy cells remains a major limitation. Efforts to design smaller peptide fragments or modified analogs have sought to preserve its antineoplastic properties while improving selectivity, yet results remain inconclusive. Given this background, the present study aims to evaluate the antitumor activity of Ctn-2, a crotalicidin-derived peptide fragment, using in vitro TNBC models, and to determine whether Ctn-2 can potentiate the cytotoxic efficacy of the standard chemotherapeutic agent doxorubicin.

## 2. Materials and Methods

### 2.1. Cell Cultures

The human cell line MDA-MB-231 (CRM-HTB-26, ATCC, Manassas, VA, USA), derived from triple-negative mammary adenocarcinoma, and the non-tumor human keratinocyte cell line (HaCaT) were used. The cells were cultured at 37 °C in 1:1 mixture of DMEM (11965084, Invitrogen, Carlsbad, CA, USA) and RPMI (11875093, Invitrogen, Carlsbad, CA, USA) supplemented with 10% fetal bovine serum (FCS, 12657029, Gibco, Grand Island, NY, USA), 100 µg/mL of penicillin, and 100 µg/mL of streptomycin, in a humidified atmosphere with 5% CO<sub>2</sub>. The experiments were performed with exponentially proliferating cultures and were subcultured twice a week or until they reached confluence in a monolayer.

### 2.2. Peptide and Phospholipids

The peptide Ctn-2 (KRFKKFFKKVKKSVKRLKKIFKK, Lot. U1440EE070-7/PE1320) derived from crotalicidin, a peptide identified in the venom of the *Crotalus durissus ter-rificus* snake, was generated through a rational structural design collaboratively by the University of Antioquia and University of the Andes [7]. Ctn-2 was designed to closely resemble the native sequence derived from crotalicidin, in which the C-terminus is not amidated. Preservation of the native chemical structure was essential to maintain biological relevance and to enable meaningful structure–activity relationship comparisons with the parent peptide and previously reported crotalicidin-derived sequences. The peptide LTX-315 (KKWWKKWDipK–NH<sub>2</sub>, Dip: Diphenylalanine, Lot. U037QFC180-14/PE6102), whose activity in cancer has been widely reported, was used as a positive control [8]. Both peptides were obtained according to the reported sequence by the solid-phase method

and purchased from GenScript (Piscataway Township, NJ, USA). Trifluoroacetic acid removal was performed. The purity and molecular weights of the peptides were determined by HPLC (higher than 95%) and MALDI-TOF mass spectrometry, respectively. Table 1 summarizes the characteristics of the peptides used in this research.

**Table 1.** Sequence and properties of the peptides Ctn-2 and LTX-315.

Peptide	Sequence	Number of Amino Acids	Charge	Theoretical MW	% Purity
Ctn-2	KRFKFFFKVKKSVKKRLKKIFKK	24	+15	3096.98	96.8
LTX-315	KKWWKKWDipK-NH <sub>2</sub>	9	+6	1439.78	97.5

Phospholipids with 16:0 acyl chains were purchased from Avanti Polar Lipids (Alabaster, AL, USA), including: 1,2-dipalmitoyl-sn-glycero-3-phosphocholine (DPPC, Lot. 160PC-318), 1,2-dipalmitoyl-sn-glycero-3-phosphoethanolamine (DPPE, Lot. 160PE-106), 1,2-dipalmitoyl-sn-glycero-3-phospho-L-serine sodium salt (DPPS, Lot. 840037P-500MG-A-078), and sphingomyelin extracted from chicken egg (SM, Lot. 860061P-25MG-A-116). Additional reagents, including HEPES, EDTA, NaCl, and other chemicals of analytical grade, were acquired from Sigma-Aldrich (St. Louis, MO, USA).

### 2.3. Evaluation of Cytotoxicity by MTT

The Ctn-2 peptide was evaluated at a range of concentrations in the  $\mu\text{M}$  range to identify the median inhibitory concentration ( $\text{IC}_{50}$ ) and determine the cytotoxic potential and working concentrations. Cytotoxicity assays were performed with 1 h, 6 h, and 24 h treatments and at least 5 concentrations. Cell viability was quantified using the MTT (3-(4,5-dimethylthiazol-2-yl)-2,5-diphenyltetrazolium bromide) assay (475989, Sigma-Aldrich, St. Louis, MO, USA). Briefly, exponential-phase cells cultured in 96-well microplates were used. Microplates were seeded in triplicate; each experiment was performed three separate times on different days. Absorbance was measured at 570 nm using a Varioskan™ microplate reader (Thermo Fisher Scientific, Waltham, MA, USA). Untreated cells were included as negative controls in all assays. Treatments with 6% DMSO and the oncolytic peptide LTX-315 were included as positive controls. The conventional chemotherapeutic doxorubicin (44583, Sigma-Aldrich, St. Louis, MO, USA) was then evaluated at concentration ranges in the  $\mu\text{M}$  scale to identify the mean inhibitory concentration ( $\text{IC}_{50}$ ), and thereby determine the cytotoxic potential and working concentrations. Cytotoxicity assays of the combination of Doxo and the Ctn-2 peptide were performed with 24 h treatments, covering a single concentration close to the  $\text{IC}_{50}$  of Doxo in cotreatment with different doses of the peptide in the  $\mu\text{M}$  range. Cell viability was quantified using the MTT assay as previously described. The selectivity index is calculated using the following equation:

$$SX = \frac{\text{IC}_{50 \text{ non-tumoral cell}}}{\text{IC}_{50 \text{ tumoral cell}}} \times 100$$

### 2.4. Phase Transition Experiments of Model Membranes by Infrared Spectroscopy

20 mM lipid stock solutions of the representative multi-component lipid systems HaCaT, DPPC/DPPE/SM 59:35:6 (*w/w*) and MDA-MB-231, DPPC/DPPE/SM/DPPS 43:33:4:20 (*w/w*) were prepared in chloroform and stored at  $-20\text{ }^{\circ}\text{C}$ . Lipid transition measurements were performed in the BioATR II cell from the Tensor II spectrometer (Bruker Optics, Ettlingen, Germany) using an MCT (Mercury, Cadmium, Tellurium) detector, a spectral resolution greater than  $0.4\text{ cm}^{-1}$ , and 120 scans per measured temperature. The cell was connected to a Huber Ministat 125 circulating water bath (Huber, Offenburg, Germany) that controls the required temperature with  $\pm 0.01\text{ }^{\circ}\text{C}$  accuracy. For the phase

transition 20  $\mu\text{L}$  of 20 mM HEPES pH 7.4 buffer was added directly to the silicon crystal of the cell to record the background in a programmed temperature ramp range from 40 to 65  $^{\circ}\text{C}$  with a heating rate of 1  $^{\circ}\text{C}/\text{min}$  and equilibration time of 120 s between each measurement. After recording the background, the supported lipid bilayers (SLBs) were prepared in situ on the crystal by adding 20  $\mu\text{L}$  of the 20 mM lipid stock solution, the solvent was evaporated, and the lipid multilayer film was hydrated using 20  $\mu\text{L}$  of the same buffer at 60  $^{\circ}\text{C}$  for 10 min for both lipid systems. Then, the samples were analyzed under the same temperature range set as the background. During hydration, 1, 5, and 10 molar% of Ctn-2 peptide were added in the same buffer.

Data processing was carried out using the OPUS 3D 8.8.4 software (Bruker Optics, Ettlingen, Germany), which automatically subtracted the background from each recorded sample. The main phase transition temperature ( $T_m$ ) was analyzed via the vibration of methylene groups (2970 to 2820  $\text{cm}^{-1}$ ). For this, the frequency range of the symmetric extension (2850 to 2853  $\text{cm}^{-1}$ ) was cut from the spectra with subsequent baseline correction using the 20% sensitivity rubber band method. The maximum wavenumber for the symmetric extension of each temperature was obtained using the peak-picking tool. The same procedure was performed to analyze the hydration at the phospholipid interface region via the ester carbonyl stretching vibration around 1725 to 1740  $\text{cm}^{-1}$ . Finally, the data were plotted as a wavenumber as a function of temperature, and to determine  $T_m$ , the experimental sigmoidal curve was fitted into a Boltzmann function with a Levenberg–Marquardt iteration algorithm to calculate the inflection point of the curve using the Origin Pro 8.0 software (OriginLab Corporation, Northampton, MA, USA) [9].

### 2.5. LDH Release

Following the manufacturer's instructions, cell membrane disruption induced by the peptide Ctn-2 was evaluated using the CytoTox-ONE™ Homogeneous Membrane Integrity Assay (G7892, Promega Corporation, Madison, WI, USA).  $1 \times 10^4$  cells were seeded in a 96-well plate and treated with Ctn-2 at various concentrations ( $\mu\text{M}$ ) for 24 h. To ensure 100% LDH release, 2  $\mu\text{L}$  of Lysis Solution (G1828, Promega Corporation, Madison, WI, USA) were added to the designated wells per 100  $\mu\text{L}$  of culture medium. After treatment, the supernatants were identified. Fluorescence was recorded at 570 nm using a Varioskan™ microplate reader (Thermo Fisher Scientific, Waltham, MA, USA). The data were expressed as:

Percentage of LDH release:

$$\% \text{ LDH release} = \frac{\text{Experimental fluorescence}}{\text{Maximum LDH release fluorescence}} \times 100$$

### 2.6. Evaluation of PI Uptake and Mitochondrial Membrane Potential

To simultaneously assess plasma membrane integrity and mitochondrial transmembrane potential ( $\Delta\psi_m$ ), cells were stained using a mixed-dye solution containing Propidium Iodide (PI, P4170, Sigma-Aldrich, St. Louis, MO, USA) and DiOC<sub>6</sub> (D273, Molecular Probes, Eugene, OR, USA). After exposure to the peptide, the cells were resuspended in 300  $\mu\text{L}$  of PBS containing 50 nm of DiOC<sub>6</sub> and 0.30  $\mu\text{g}/\text{mL}$  of PI and incubated in the dark at room temperature for 30 min. Following incubation, the samples were analyzed using a BD LSRFortessa flow cytometer (Franklin Lakes, NJ, USA). PI fluorescence was used to quantify membrane permeabilization, while the DiOC<sub>6</sub> signal was evaluated to determine changes in  $\Delta\psi_m$ .

### 2.7. Detection of Intracellular ROS

It was sought to determine whether the peptide has the capacity to increase oxidative stress, which can generate variations in intracellular concentrations of reactive oxygen species (ROS), thus modulating its antitumor effect. For this, cells were seeded in 6-well plates for 24 h to allow their growth and were treated with different concentrations of peptide. After treatments, the cells were disrupted and exposed to MitoTracker Red CM-H2Xros (M7513, Invitrogen, Carlsbad, CA, USA) for 15 min and incubated at 37 °C, subsequently washed three times with PBS, and analyzed using a BD LSRFortessa flow cytometer (Franklin Lakes, NJ, USA).

### 2.8. Assessment of Membrane Integrity and Phosphatidylserine Exposure

Apoptosis Detection Kit (V35112, Invitrogen, Carlsbad, CA, USA) was used. Exponentially growing cells were seeded in 6-well microplates after allowing cell adhesion, the peptide was added and after the treatment time, a single 15-min staining step was performed (in the dark) following the kit manufacturer's instructions. Quantification was done by flow cytometry in channel FL1 for Annexin (488/350 nm) and in FL2 for Sytox Green, the latter to differentiate necrotic cells. The flow cytometer automatically analyzes 10,000 events (cells) per sample (well).

### 2.9. Statistical Analysis

Statistical analysis and graphs were performed using GraphPad Prism (version 8.0.2 for Windows). Experiments were performed in triplicate and after calculating the mean, comparisons between datasets were made using one-way or two-way analysis of variance (ANOVA), as appropriate, followed by a post hoc test. Data are presented as mean  $\pm$  standard error of the mean (SEM), with a  $p$ -value  $\leq 0.05$  considered statistically significant.

## 3. Results

### 3.1. Ctn-2 Reduces Cell Viability in TNBC Cells and Shows Tumor Selectivity

The cytotoxic effect of Ctn-2 was assessed in MDA-MB-231 triple-negative breast cancer cells and in non-tumoral HaCaT cells following treatment with 0, 6.25, 12.5, 25, and 50  $\mu$ M for 1, 6, and 24 h. IC<sub>50</sub> values were determined using the MTT assay, and LTX-315 was included as a positive control in the MDA-MB-231 experiments. Figure 1a,b show the responses of MDA-MB-231 and HaCaT cells, respectively, both exhibiting a dose- and time-dependent reduction in viability. Figure 1c illustrates the cytotoxic effect of LTX-315 in MDA-MB-231 cells, which also displayed a dose-dependent pattern; however, Ctn-2 consistently demonstrated greater potency in the tumor cell line compared with the control peptide. Notably, Ctn-2 produced a significant decrease in viability at concentrations of 25  $\mu$ M and above across all time points in the TNBC cells.

Table 2 summarizes the IC<sub>50</sub> values obtained for Ctn-2 and the control peptide LTX-315. In MDA-MB-231 cells, Ctn-2 exhibited an IC<sub>50</sub> of 27.58  $\mu$ M at 24 h, which is lower than that of LTX-315 (47.84  $\mu$ M), indicating greater cytotoxic potency in the TNBC cell line. Ctn-2 was consistently less cytotoxic in the non-tumoral HaCaT cells, highlighting its preferential activity toward tumor cells. The IC<sub>50</sub> values showed minimal variation across 1, 6, and 24 h, suggesting that the cytotoxic effect is largely time-independent. Overall, the high selectivity indices obtained (SI 96–161) demonstrate that Ctn-2 selectively targets TNBC cells while exerting substantially lower toxicity on non-tumoral cells. Accordingly, concentrations of 7.5, 15, and 30  $\mu$ M at 24 h were selected for subsequent experiments.

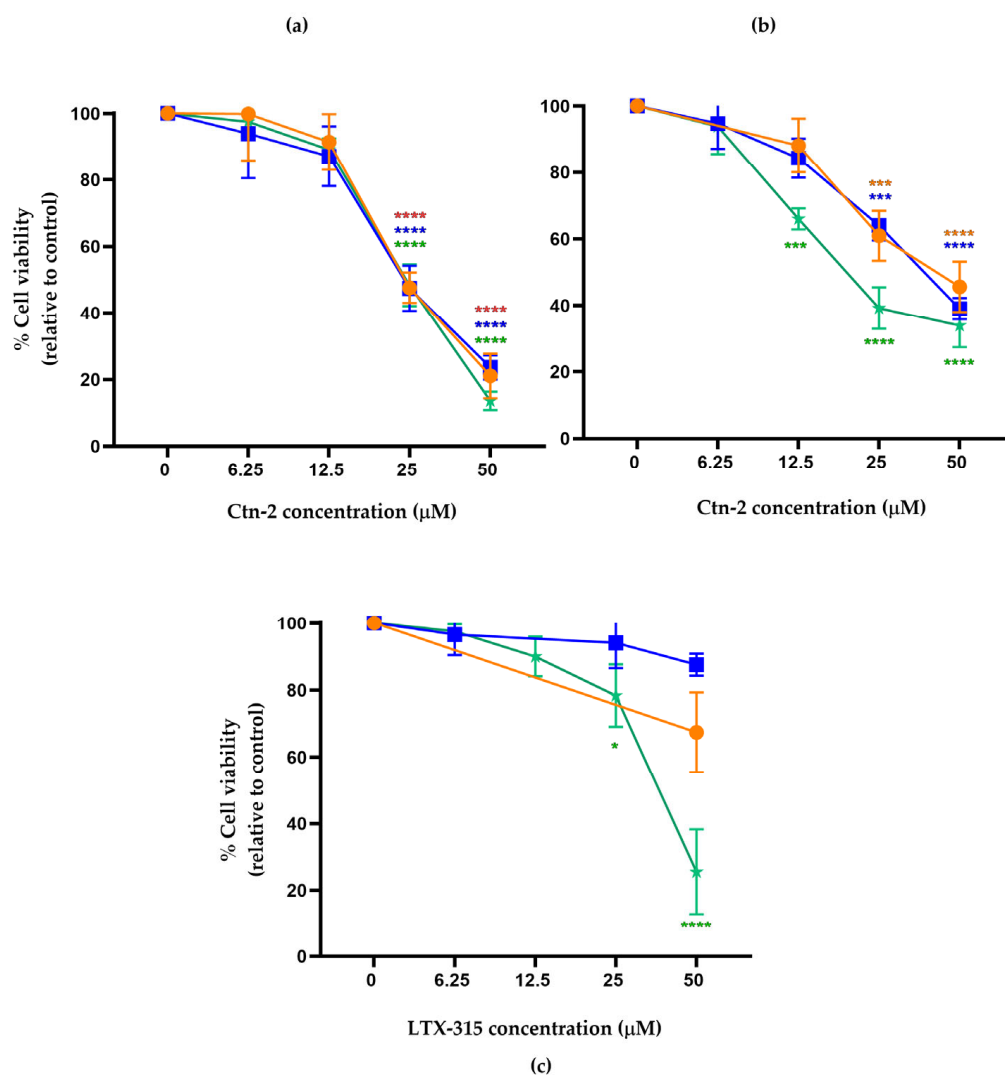


**Figure 1.** Cytotoxicity induced by Ctn-2 and LTX-315 in MDA-MB-231 and HaCaT cell lines. (a) Ctn-2 in MDA-MB-231 cells, (b) Ctn-2 in HaCaT cells, and (c) LTX-315 in MDA-MB-231 cells. Cells were treated with different peptide concentrations for 1 h (●), 6 h (■), and 24 h (\*). Cytotoxicity was assessed using MTT. Untreated cells were considered to have 100% viability. Data are expressed as mean ± SEM from at least three independent experiments. Statistical analysis was performed using two-way ANOVA; differences with respect to NT, \*  $p < 0.05$  and \*\*\*  $p < 0.001$  and \*\*\*\*  $p \leq 0.0001$ .

**Table 2.** Half-maximal inhibitory concentrations ( $IC_{50}$ ) of the peptide Ctn-2 and LTX-315 on non-tumoral HaCaT cells, and breast cancer cells MDA-MB-231. The selectivity index (SX) was calculated for MDA-MB-231 cells.

Time (h)	Ctn-2 $IC_{50}$ (μM)		LTX-315 $IC_{50}$ (μM)	Ctn-2
	MDA-MB-231	HaCaT	MDA-MB-231	Selectivity Index (SX) *
1	32.84	52.90	211.3	161
6	30.96	43.96	388.1	142
24	27.58	26.60	47.84	96.4

\* SX value > 100 denotes that the cytotoxic effect is more selective in cancer cells [10].

### 3.2. Ctn-2 Interacts Selectively with Lipid Components of Tumoral Membranes

Given that many anticancer peptides exert their activity through direct interactions with the phospholipids of the plasma membrane, we next investigated whether Ctn-2 differentially interacts with lipid constituent's characteristic of tumoral versus non-tumoral

membranes. To monitor this interaction, Fourier Transformed infrared spectroscopy (FT-IR) was used. FTIR spectroscopy was selected as it enables sensitive monitoring of lipid phase behavior and structural dynamics in model membranes. This technique probes vibrational modes arising from key bilayer region, including acyl chains and ester carbonyls groups, providing insight into changes in lipid organization. In particular, the  $\nu_s\text{CH}_2$  band serves as a robust indicator of acyl-chain conformational order, allowing the detection of phase transitions through temperature-dependent shifts between the gel ( $L\beta$ ) and liquid-crystalline ( $L\alpha$ ) phases. Increases in wavenumber reflect enhanced chain disorder and membrane fluidization, enabling precise determination of the  $T_m$ . Examples of individual spectra of the controls and in the presence of the highest concentration of Ctn (10 mol%) are summarized in Figures S1–S4.

Because antimicrobial peptides interact first with the membrane surface, we also examined the interfacial and headgroup regions. The C=O stretching vibration is highly responsive to alterations in hydrogen bonding, hydration, and headgroup conformation, all of which may occur upon peptide binding or insertion. This  $\nu\text{C}=\text{O}$  band, typically found between  $1760$  and  $1700\text{ cm}^{-1}$ , provides a sensitive indicator of changes at the polar–apolar interface. Downshifts indicate increased hydrogen bonding or a more polar environment, whereas upshifts denote dehydration or structural perturbation of the interface induced by peptide–membrane interactions. The analysis of the results showed that Ctn-2 did not induce alterations on the non-tumoral membrane model (Figure 2a), indicating an absence of detectable peptide–lipid interaction.

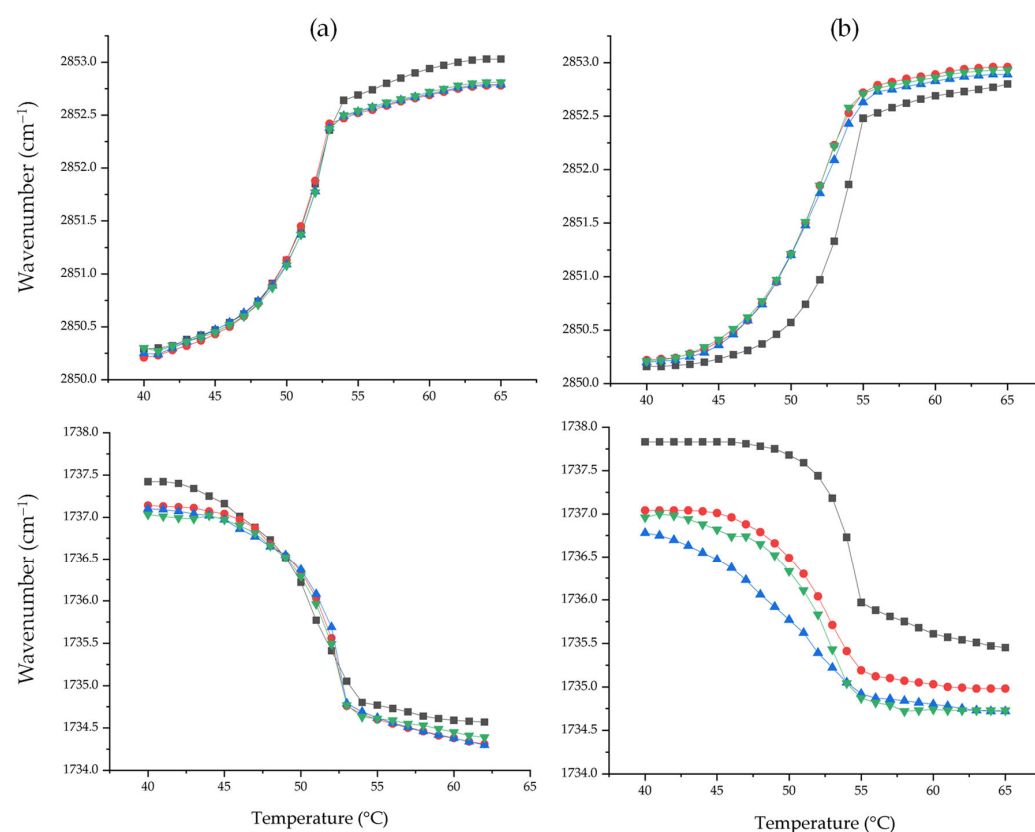


**Figure 2.** Peak positions of the symmetric methylene stretching ( $\nu_s\text{CH}_2$ , top panels) and carbonyl stretching ( $\nu\text{C}=\text{O}$ , bottom panels) bands of non-tumoral (a) and tumoral membranes (b) in the absence of peptide (■) and presence of increasing concentrations (1%, 5%, 10%) of Ctn-2. Symbols correspond to different peptide concentrations: 1% (●), 5% (▲), and 10% (△). All spectra were recorded in buffer (20 mM HEPES at pH 7.4).

In contrast, pronounced spectral changes were observed in the tumoral membrane model (Figure 2b). Increasing concentrations of Ctn-2 induced a reduction of the  $T_m$  in a non-concentration effect, indicating acyl chain disorder during the gel-to-liquid crystalline transition. However, analysis of the  $\nu C=O$  band showed a different tendency. Increasing concentrations of the peptides induced a gradual downshift of the carbonyl vibration related to a more polar environment. These results are consistent with a direct interaction between Ctn-2 and cancer-associated lipids. This effect could suggest that Ctn-2 has an intrinsic affinity for the altered biophysical properties of tumor cell membranes rather than exhibiting a purely dose-dependent interaction. These findings support the selectivity observed in the cytotoxic assays and highlight membrane targeting as a central component of the mechanism of action of Ctn-2.

### 3.3. Ctn-2 Induces Controlled Membrane Permeabilization and Promotes ROS Accumulation in TNBC Cells

After establishing that Ctn-2 selectively interacts with lipids from tumor membranes, we investigated whether this interaction leads to partial membrane permeabilization or complete membrane disruption. To assess plasma membrane integrity, two complementary assays were performed: propidium iodide (PI) uptake, which detects loss of membrane integrity, and lactate dehydrogenase (LDH) release, which indicates overt membrane rupture and cytosolic leakage. Figure 3a shows that PI uptake increased progressively with increasing Ctn-2 concentration, demonstrating that the peptide compromises membrane integrity and allows the passage of small, normally impermeant molecules. This graded response is consistent with the disruption of the membrane rather than immediate lysis. In agreement with this observation, LDH release (Figure 3b) also increased in a concentration-dependent manner.

Given that membrane perturbation can trigger intracellular stress responses, mitochondrial function was assessed. Measurements of mitochondrial membrane potential ( $\Delta\Psi_m$ ) using DiOC<sub>6</sub>(3) are shown in Figure 3a. The data revealed no significant changes across the tested concentrations, indicating that Ctn-2 does not compromise mitochondrial membrane integrity or induce depolarization under these conditions. In contrast, mitochondrial ROS levels increased in a concentration-dependent manner in the present study (Figure 3c). The increase in ROS, despite preserved  $\Delta\Psi_m$ , suggests that mitochondrial stress occurs without structural collapse, likely as a secondary consequence of plasma membrane perturbation rather than direct mitochondrial damage.

### 3.4. Ctn-2 Does Not Affect the Localization of Phosphatidylserine in the Cytoplasmic Membrane in MDA-MB-231 Cells

To determine whether the membrane permeabilization and oxidative stress induced by Ctn-2 led to apoptotic cell death, we evaluated phosphatidylserine (PS) exposure on the cell surface. MDA-MB-231 cells were treated with different doses (0  $\mu$ M, 7.5  $\mu$ M, 15  $\mu$ M, and 30  $\mu$ M) of the peptide Ctn-2 for 24 h. Doxorubicin at a concentration of 2.5  $\mu$ M was included as a control. The results are shown in Figure 4, where a dose-dependent relative increase in fluorescence intensity is observed. However, in contrast to the doxorubicin control, whose primary cell death mechanism is known to be apoptosis, the fluorescence observed in the Ctn-2-treated cells is not indicative of apoptosis.

### 3.5. Combined Treatment of Ctn-2 and Doxorubicin Enhances Cytotoxicity in MDA-MB-231 Cells

Given that Ctn-2 induces selective plasma membrane permeabilization in TNBC cells, we hypothesized that this disruption could facilitate the intracellular uptake of conventional chemotherapeutics. To determine whether Ctn-2 enhanced the efficacy of standard treatment, MDA-MB-231 cells were exposed to doxorubicin either alone or in combination

with the subtoxic concentration of Ctn-2 (15  $\mu\text{M}$ ). Combination treatments were performed using both pre-treatment and co-treatment schemes, as outlined in Figure 5a. Cell viability was quantified using the MTT assay to determine the  $\text{IC}_{50}$  of doxorubicin under each condition. The corresponding results are shown in Figure 5b.

The results of the different treatment regimens were compared to the control, treated only with doxorubicin. Both pre-treatment and co-treatment showed a significant difference in cell viability at all doses, with decreasing cell viability compared to monotherapy with the chemotherapy agent. These results suggest a potentiating effect of Ctn-2 on the conventional chemotherapeutic agent doxorubicin. The  $\text{IC}_{50}$  results for these combinations are included in Table 3, which compares the  $\text{IC}_{50}$  of doxorubicin alone versus the combination treatments.

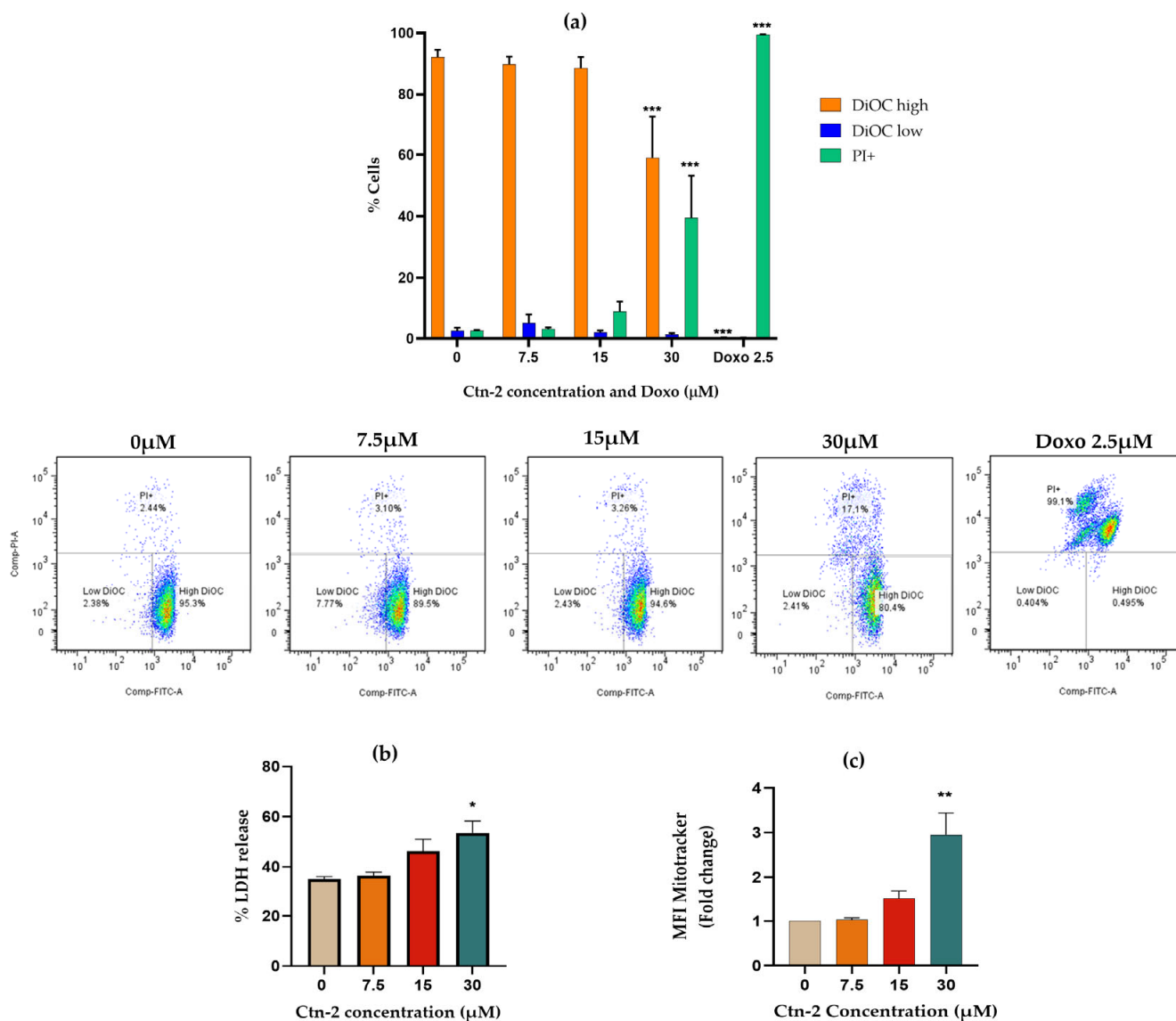


**Figure 3.** Ctn-2 permeabilizes the plasma membrane and increases ROS levels but does not induce mitochondrial membrane depolarization in MDA-MB-231 cells. MDA-MB-231 cells were treated with increasing concentrations of Ctn-2 (7.5, 15, and 30  $\mu\text{M}$ ) for 24 h and processed using different methodologies (a) Flow cytometry quantification of propidium iodide (PI) uptake and DiOC6 caption. Representative dot plots are shown below. (b) Evaluation of membrane disruption using LDH release assay (c) Mitochondrial ROS levels measured using MitoTracker Red CM-H<sub>2</sub>Xros. All data are presented as mean  $\pm$  SEM from at least three independent experiments. One-way ANOVA was used to compare the populations of untreated (0  $\mu\text{M}$ ) and treated cells. Statistical significance is denoted by \*  $p < 0.05$ , \*\*  $p < 0.01$ , and \*\*\*  $p < 0.001$ .

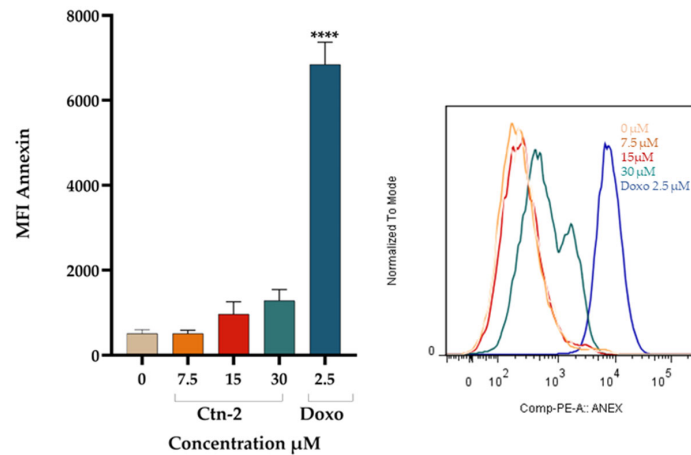


**Figure 4.** Effect of Ctn-2 peptide treatment on phosphatidylserine exposure in MDA-MB-231 cells. MDA-MB-231 cells were treated with different concentrations of Ctn-2 for 24 h and subsequently analyzed by flow cytometry using the Annexin V-PE fluorophore. The bar chart shows the mean  $\pm$  SEM of the Median Fluorescent Intensity of Annexin. The right panel shows representative histograms. Statistical analysis using one-way ANOVA revealed no significant differences compared with untreated cells. In contrast, the doxorubicin control showed a statistically significant increase in Annexin V-positive cells (\*\*\*\*  $p \leq 0.001$ ).

(a)

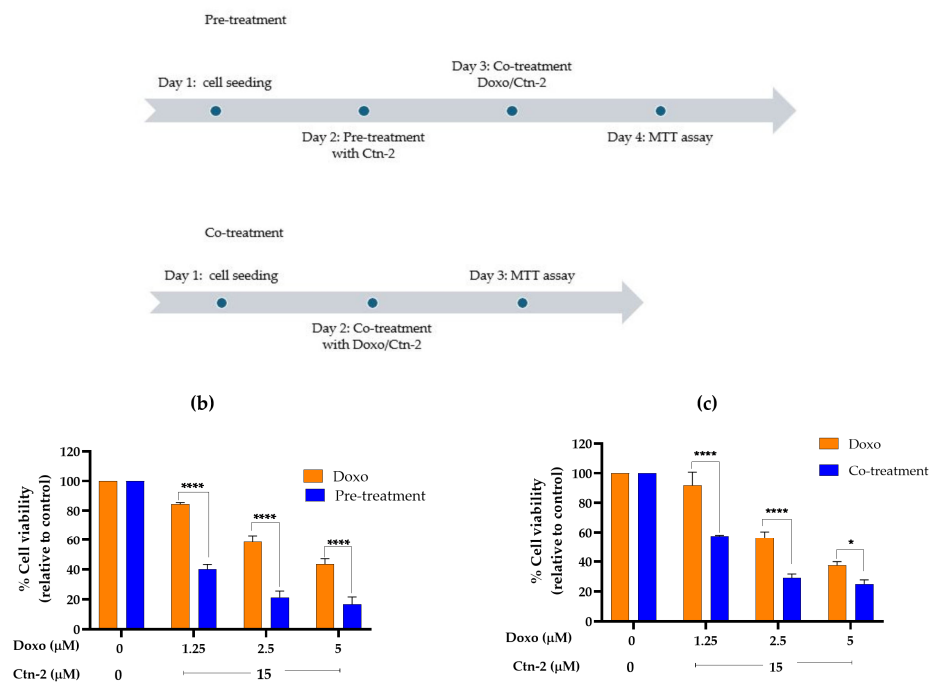


**Figure 5.** Ctn-2 Pre-treatment and co-treatment reduce the IC<sub>50</sub> of doxorubicin in MDA-MB-231 cells. MDA-MB-231 triple-negative breast cancer cells were exposed to a subtoxic concentration of Ctn-2 (15  $\mu$ M) in combination with doxorubicin (1.25  $\mu$ M, 2.5  $\mu$ M, and 5  $\mu$ M) under two treatment schemes. (a) Experimental design. In the pre-treatment scheme, cells were seeded on Day 1, treated with Ctn-2 on Day 2, followed by co-treatment with Ctn-2 and doxorubicin on Day 3; viability was assessed on Day 4 using the MTT assay. In the co-treatment scheme, cells were seeded on Day 1 and treated simultaneously with Ctn-2 and doxorubicin on Day 2; viability was measured on Day 3. Treatments with doxorubicin alone at the same concentrations were used as controls. (b) Cell viability for pre-treatment scheme, (c) Cell viability for co-treatment scheme. Data are expressed relative to untreated cells. Data represent the mean  $\pm$  SEM from three independent experiments. Statistical comparisons were performed by two-way ANOVA. Significant differences relative to untreated controls (0  $\mu$ M) are indicated as \*  $p \leq 0.05$  and \*\*\*\*  $p \leq 0.0001$ .

**Table 3.** IC<sub>50</sub> values of doxorubicin alone and in combination with Ctn-2 under pre- and co-treatment conditions in MDA-MB-231 cells.

	Pre-Treatment	Co-Treatment
Doxorubicin	4.146 $\mu$ M	3.974 $\mu$ M
Doxorubicin + Ctn-2	0.8040 $\mu$ M	1.412 $\mu$ M

#### 4. Discussion

Breast cancer is highly heterogeneous and is classified based on the tissue of origin and the expression of molecular markers like the estrogen receptor (ER), progesterone receptor (PR), and human epidermal growth factor receptor 2 (HER2) [11–14]. The subtype known as TNBC presents the most aggressive phenotype because it lacks expression of ER, PR, and HER2 receptors. This absence renders standard targeted treatments, such as hormonal therapies or specific antibodies, ineffective [15]. Consequently, conventional treatment for TNBC relies primarily on chemotherapy, often administered in combinations to prevent chemoresistance. However, TNBC rapidly acquires resistance to these conventional therapies [14–16]. Studies have shown that resistant genotypes often pre-exist and are selectively favored by chemotherapy [17–19], highlighting the urgent need for new therapeutic strategies.

Bioactive peptides have garnered interest because their mechanism of action often involves interaction with the outer cell membrane, providing a means to evade the common drug resistance mechanisms developed by tumors. These peptides exhibit biological activity and promising selectivity toward tumor cells [20,21]. Crotalicidin (Ctn) is an antimicrobial peptide isolated from the venom of the South American rattlesnake *Crotalus durissus terrificus*. Ctn is composed of a 34 amino acid sequence (KRFKFFKVKKSVKLR-LKKIFKPPMVGVTIPF) and a net charge of +15. Ctn belongs to the cathelicidin family of host defense peptides, which are widely distributed across multiple species and play essential biological roles. Depending on the organism, cathelicidins function either as key components of the immune defense system or as potent hunting and predation tools. Falcão and colleagues reported the identification of several snake venom-derived cathelicidins with antibacterial activity [22]. Among these, crotamine has demonstrated antitumor activity by penetrating cells and interacting with intracellular targets to promote cytotoxic effects. Crotalicidin has also been shown to exhibit potent lethal activity against a variety of microorganisms [23].

Ctn has been reported to exhibit broad-spectrum activity against ATCC strains and clinical isolates of several Gram-positive and Gram-negative bacterial species [24]. In addition, its potential antitumor activity has been explored in recent studies. Falcão and colleagues characterized the secondary structure of Ctn, which consists of an N-terminal  $\alpha$ -helical region and an unstructured C-terminal region. They also evaluated the cytotoxic activity of two Ctn-derived fragments, Ctn(1–14), which retains the  $\alpha$ -helical structure but loses cytotoxicity in both bacterial and tumor cell models, and Ctn(15–34), which maintains cytotoxic activity in both models, although at lower levels than full-length Ctn and with slightly improved selectivity toward eukaryotic cells [24]. Despite its antitumor potential, Ctn is moderately hemolytic and unstable in serum, which increases its cytotoxicity, also affecting healthy cells. Although Ctn and Ctn(15–34) have shown antitumor activity, it is still necessary to investigate which peptide fragments can be identified as having active motifs with improved and more selective properties in eukaryotic cells.

The Ctn-2 peptide is a synthetic fragment derived from Ctn. It was specifically synthesized to be more active and less toxic than the original Ctn, and it retains a high net charge (+15) and key amphipathic properties important for interacting with biological

membranes. In this study, we evaluated the cytotoxic properties of Ctn-2 against triple-negative breast cancer cells. Our findings demonstrate that Ctn-2 exhibits potent antitumor activity against MDA-MB-231 cells while maintaining clear selectivity over non-tumorigenic HaCaT keratinocytes. Notably, Ctn-2 displayed an  $IC_{50}$  of 27.58  $\mu\text{M}$  at 24 h, breaking the reference oncolytic peptide LTX-315 ( $IC_{50} = 36.3 \mu\text{M}$ ). Importantly, the selectivity index (SI) of Ctn-2 ranged from 96 to 161, indicating a strong preference for malignant cells and supporting its potential as a tumor-selective therapeutic candidate.

Using Fourier-transform infrared spectroscopy, it was possible to evaluate the affinity of Ctn-2 to the lipids present in the cancer membrane model. The results showed a preference for the tumoral over the non-tumoral model. It is widely recognized that the cytotoxic mechanism of BAPs is driven primarily by electrostatic interactions between their cationic amino acid residues and the anionic constituents of cancer cell membranes. In malignant cells, an increased surface exposure of negatively charged lipids, most prominently phosphatidylserine (PS), along with sialylated gangliosides, O-glycosylated mucins, and heparan sulfates, accounts for their heightened susceptibility to cationic peptides [25–27]. Among the model membranes evaluated, the principal distinguishing feature of the tumor-mimetic system was the incorporation of PS. This anionic phospholipid could significantly enhance the electrostatic attraction of Ctn-2 toward tumor-like bilayers, thereby contributing to its preferential interaction with, and potential selectivity for, cancer cells.

In vitro assays carried out to evaluate the cellular membrane integrity demonstrated that propidium iodide uptake increased progressively with Ctn-2 concentration, confirming the compromising of membrane integrity and the passage of small molecules. This disruption is characterized as a controlled permeabilization rather than a complete, immediate membrane rupture (lysis). While the release of cytosolic content, measured by lactate dehydrogenase (LDH) release, was observed, its magnitude was lower than expected for full membrane breakdown.

Regarding subsequent intracellular effects, Ctn-2 treatment leads to a concentration-dependent increase in mitochondrial ROS. Importantly, this ROS accumulation occurs despite the preservation of mitochondrial membrane potential ( $\Delta\Psi_m$ ), indicating that Ctn-2 does not directly compromise mitochondrial integrity or induce depolarization under these conditions. Therefore, the mitochondrial stress is likely a secondary consequence of the primary plasma membrane perturbation. Furthermore, Ctn-2 does not appear to induce apoptosis, as it did not significantly increase phosphatidylserine exposure (Annexin V positivity) compared to the doxorubicin control.

These results are consistent with previous reports describing membrane-centric mechanisms for Crotalicidin and its derivatives. Pérez-Peinado et al. demonstrated that both full-length Ctn and its C-terminal fragment Ctn(15–34) permeabilize bacterial membranes through a three-step process: initial electrostatic attraction, peptide accumulation at the surface, and subsequent membrane lysis [28]. Similarly, another study reported that these peptides preferentially disrupt tumor cell membranes and can additionally interact with intracellular pathways, contributing to necrotic or apoptotic cell death [29]. Klais-Luna et al. published an approach to the mechanism of action of Ctn related to TNBC. This study used biophysical techniques to investigate the mechanism of the peptide at the membrane level. The results suggested that the process begins with the electrostatic interaction of the peptide with the surface of the lipid bilayer, followed by a conformational change and the intercalation of the peptide between the lipid chains of negatively charged phospholipids [21]. Carrera-Aubesart et al. synthesized and analyzed topoisomers of Ctn and its C-terminal fragment Ctn(15–34) using Gram-negative bacteria and various tumor cell lines. They explored the structural and

functional properties of these topoisomers. The results showed that the Ctn topoisomers exhibited superior antitumor activity to Ctn(15–34) analogs, primarily in tumor cell lines. However, they retained cytotoxic effects in non-tumor cells. They concluded that the efficacy of these peptides depends on specific electrostatic interactions with respect to negatively charged membranes rather than their secondary structural conformation [30]. Finally, Gallego-Londoño et al. recently evaluated the cytotoxic activity of the peptides Ctn and NA-CATH-ATRA-1-ATRA-1 (identified in the snake *Naja atra*) in the breast cancer cell lines MCF-7 and MDA-MB-231 [31]. The results showed that both peptides possess potent cytotoxicity, mainly through membranolytic mechanisms, and show promising efficacy in targeting cancer cells. However, the levels of cytotoxicity for non-tumor cells remain high.

Our findings are consistent with previous studies and further expand on them by demonstrating, for the first time, that Ctn-2 retains this selective membranolytic behavior in triple-negative breast cancer cells. Unlike earlier Ctn variants, which are known to produce strong lytic effects along with cytotoxicity and low selectivity toward non-tumor cells, Ctn-2 induces controlled membrane permeabilization rather than immediate lysis. Moreover, when evaluated in the non-tumor HaCaT cell line, the results showed selectivity compared with the tumor cell line, highlighting an improved therapeutic profile and supporting the development of Ctn-2 as a membrane-active peptide with tumor selectivity.

Given that Ctn-2 selectively permeabilizes the plasma membrane of MDA-MB-231 cells, we hypothesized that this disruption could facilitate the intracellular uptake of traditional chemotherapeutics. In this regard, doxorubicin is one of the most widely used chemotherapeutic agents for breast cancer. As an anthracycline, its cytotoxic mechanism relies on DNA intercalation and inhibition of topoisomerase II [32]. Despite its clinical value, doxorubicin is associated with serious adverse effects, such as its high cardiotoxicity [33]. In addition, various mechanisms confer specific resistance to this treatment in breast cancer [20,21,34]. Consistent with this hypothesis, combining a subtoxic dose of Ctn-2 (15  $\mu\text{M}$ ) with doxorubicin markedly potentiated its cytotoxic action in MDA-MB-231 cells. Ctn-2 reduced the  $\text{IC}_{50}$  of doxorubicin from 4.146  $\mu\text{M}$  under single-agent treatment to 0.8040  $\mu\text{M}$  in the pre-treatment combination. A similar increase in sensitivities was observed in the co-treatment scheme, demonstrating a consistent chemosensitizing effect. These findings indicate that Ctn-2 can significantly amplify the therapeutic activity of doxorubicin, likely by facilitating its cellular entry through membrane destabilization. This combinatorial strategy may therefore represent a promising approach to enhance drug efficacy, reduce required anthracycline doses, and potentially mitigate systemic toxicity in the treatment of TNBC.

Bioactive peptides could represent an alternative to enhance conventional treatments, helping to reduce side effects and even lower the risk of chemoresistance. They offer a wide range of options for use in combination with traditional therapy, for example, helping to target therapy towards specific targets such as peptide-drug conjugates, immunogenic changes in the tumor microenvironment, and even interacting with specific pathways [25,35]. Vale N et al. evaluated cationic antimicrobial peptides (CAMPs) and cell-penetrating peptides (CPPs), in combination with the chemotherapeutic agent 5-FU, in the A549, UM-UC-5, and RC-5 cell lines [36]. They also assessed ADMET properties. Both *in silico* and *in vitro* cytotoxicity results showed potential for improving therapy, with various underlying mechanisms, primarily interaction with proteins involved in drug metabolism. Yamazaki et al. conducted a study with the peptide LTX-315, which has shown antitumor activity by generating immunogenic changes in the tumor microenvironment. The researchers combined LTX-315 with the anti-CTLA-4 antibody, which helps improve the immune response. They used murine

models of sarcoma and melanoma and administered the treatments intratumorally. They monitored the treated models compared to the untreated models, as well as the changes in immune cell populations. The antitumor activity of the combination therapy was more effective than monotherapies, with LTX-315 inducing the leakage of tumor cells [37]. Raileanu et al. used 3D models to evaluate the combination of doxorubicin with the antimicrobial peptide gramicidin A. They used HT-29 colorectal cancer cell spheroids, treating them at 24 and 48 h with both individual and combination therapies. The results showed decreases in cell viability and ATP levels with the combination treatments, thus demonstrating a possible potentiating effect on conventional therapy [38]. Among the mechanisms described for how peptides enhance conventional treatments, our results suggest an additional pathway by which Ctn-2 can potentiate these therapies. This makes Ctn-2 a promising subject for further investigation to support the use of this peptide for the development of less aggressive and more effective anticancer drugs.

## 5. Conclusions

Ctn-2 is a highly promising membrane-active peptide with potent and selective cytotoxicity against MDA-MB-231 cells. The peptide acts through a controlled membrane-centric mechanism supported by its selective interaction with tumor-like lipid environments, leading to progressive plasma membrane permeabilization. Intracellularly, Ctn-2 shows a distinctive response characterized by increased mitochondrial reactive oxygen species without triggering classical apoptotic pathways. Importantly, this membrane-modulating activity enhances the intracellular uptake and efficacy of conventional chemotherapeutics, supporting its potential as a chemosensitizer. Together, these findings highlight Ctn-2 as a candidate for development as a tumor-selective therapeutic and as an effective adjunct to standard TNBC treatment strategies.

**Supplementary Materials:** The following supporting information can be downloaded at: <https://www.mdpi.com/article/10.3390/scipharm94010017/s1>, The Supplementary Materials contain representative FT-IR spectra of tumoral and non-tumoral model membranes with and without Ctn-2. Figure S1: FT-IR spectra of Non-tumoral system (DPPC/DPPE/SM 59:35:6, mol%) hydrated with buffer Hepes 20 mM, pH 7.4 at 60 °C. Figure S2: FT-IR spectra of Non-tumoral system (DPPC/DPPE/SM 59:35:6, mol%) hydrated with Ctn-2 at 10 mol% in buffer Hepes 20 mM, pH 7.4 at 60 °C. Figure S3: FT-IR spectra of tumoral system (DPPC/DPPE/SM 59:35:6, mol%) hydrated with buffer Hepes 20 mM, pH 7.4 at 60 °C. Figure S4: FT-IR spectra of tumoral system (DPPC/DPPE/SM 59:35:6, mol%) hydrated with Ctn-2 at 10 mol% in buffer Hepes 20 mM, pH 7.4 at 60 °C.

**Author Contributions:** A.M.S.: investigation, writing—original draft preparation and formal analysis; M.M.-M.: experimental design, writing—review and editing; S.E.-G.: investigation; G.A.S.-G.: funding acquisition, experimental design, writing—review and editing, and project administration. All authors have read and agreed to the published version of the manuscript.

**Funding:** This research was supported by the Instituto Tecnológico Metropolitano and University of Antioquia (Grant P-23208).

**Institutional Review Board Statement:** Not applicable.

**Informed Consent Statement:** Not applicable.

**Data Availability Statement:** The original contributions presented in the study are included in the article/Supplementary Material further inquiries can be directed to the corresponding authors.

**Acknowledgments:** The authors would like to thank Engineer Esneyder Arias Cuartas for his technical assistance in the Laboratorio de Ciencias Biomédicas-ITM.

**Conflicts of Interest:** The authors declare no conflicts of interest.

## Abbreviations

The following abbreviations are used in this manuscript:

5-FU	5-fluorouracil
BC	Breast cancer
CAMPs	Cationic antimicrobial peptides
CPPs	Cell-penetrating peptides
Ctn	Crotalicidin
$\Delta\psi_m$	mitochondrial membrane potential
DMEM	Dulbecco's modified eagle medium cell culture
Doxo	Doxorubicin
ER	Estrogen receptor
FBS	Fetal bovine serum
FTIR	Fourier-transform infrared
HER2	Human Epidermal Growth Factor Receptor 2
IARC	The International Agency for Research on Cancer
IC50	Inhibitory concentration
LDH	Lactate dehydrogenase
MTT	3-(4,5-dimethylthiazol-2-yl)-2,5-diphenyltetrazolium bromide
PBS	Phosphate-buffered saline
PI	Propidium Iodide
PR	Progesterone receptor
PS	Phosphatidylserine
RPMI	Roswell Park Memorial Institute medium cell culture
SI	Selectivity Index
TNBC	Triple-negative breast cancer

## References

1. Ferlay, J.; Ervik, M.; Lam, F.; Laversanne, M.; Colombet, M.; Mery, L.; Piñeros, M.; Znaor, A.; Soerjomataram, I.; Bray, F. Cancer Observatory: Cancer Today. Lyon, France: International Agency for Research on Cancer. 2024. Available online: <https://gco.iarc.who.int/today> (accessed on 17 October 2024).
2. Derakhshan, F.; Reis-Filho, J.S. Pathogenesis of Triple-Negative Breast Cancer. *Annu. Rev. Pathol.* **2022**, *17*, 181–204. [[CrossRef](#)]
3. Won, K.; Spruck, C. Triple-negative breast cancer therapy: Current and future perspectives (Review). *Int. J. Oncol.* **2020**, *57*, 1245–1261. [[CrossRef](#)] [[PubMed](#)]
4. Ghaly, G.; Tallima, H.; Dabbish, E.; ElDin, N.B.; El-Rahman, M.K.A.; Ibrahim, M.A.A.; Shoeib, T. Anti-Cancer Peptides: Status and Future Prospects. *Molecules* **2023**, *28*, 1148. [[CrossRef](#)] [[PubMed](#)]
5. Parchebafi, A.; Tamanaee, F.; Ehteram, H.; Ahmad, E.; Nikzad, H.; Kashani, H.H. The dual interaction of antimicrobial peptides on bacteria and cancer cells; mechanism of action and therapeutic strategies of nanostructures. *Microb. Cell Factories* **2022**, *21*, 118. [[CrossRef](#)] [[PubMed](#)]
6. Pérez-Peinado, C.; Defaus, S.; Andreu, D. Hitchhiking with Nature: Snake Venom Peptides to Fight Cancer and Superbugs. *Toxins* **2020**, *12*, 255. [[CrossRef](#)]
7. Rengifo, K.R. *Actividad de Péptidos Antimicrobianos Derivados de Crotalicidina Sobre Sistemas Modelo y con Insaturaciones*; Universidad de los Andes: Bogota, Colombia, 2022.
8. Spicer, J.; Marabelle, A.; Baurain, J.-F.; Jepsen, N.L.; Jøssang, D.E.; Awada, A.; Kristeleit, R.; Loirat, D.; Lazaridis, G.; Jungels, C.; et al. Safety, Antitumor Activity, and T-cell Responses in a Dose-Ranging Phase I Trial of the Oncolytic Peptide LTX-315 in Patients with Solid Tumors. *Clin. Cancer Res.* **2021**, *27*, 2755–2763. [[CrossRef](#)]
9. Hilchie, A.L.; Doucette, C.D.; Pinto, D.M.; Patrzykat, A.; Douglas, S.; Hoskin, D.W. Pleurocidin-family cationic antimicrobial peptides are cytolytic for breast carcinoma cells and prevent growth of tumor xenografts. *Breast Cancer Res.* **2011**, *13*, R102. [[CrossRef](#)]
10. Popiołkiewicz, J.; Polkowski, K.; Skierski, J.S.; Mazurek, A.P. In vitro toxicity evaluation in the development of new anticancer drugs—Genistein glycosides. *Cancer Lett.* **2005**, *229*, 67–75. [[CrossRef](#)]
11. Hanker, A.B.; Sudhan, D.R.; Arteaga, C.L. Overcoming Endocrine Resistance in Breast Cancer. *Cancer Cell* **2020**, *37*, 496–513. [[CrossRef](#)]

12. Li, Z.; Wei, H.; Li, S.; Wu, P.; Mao, X. The Role of Progesterone Receptors in Breast Cancer. *Drug Des. Dev. Ther.* **2022**, *16*, 305–314. [[CrossRef](#)]
13. Howlader, N.; Altekruse, S.F.; Li, C.I.; Chen, V.W.; Clarke, C.A.; Ries, L.A.; Cronin, K.A. US incidence of breast cancer subtypes defined by joint hormone receptor and HER2 status. *J. Natl. Cancer Inst.* **2014**, *106*, dju055. [[CrossRef](#)]
14. Harbeck, N. Neoadjuvant and adjuvant treatment of patients with HER2-positive early breast cancer. *Breast* **2022**, *62*, S12–S16. [[CrossRef](#)] [[PubMed](#)]
15. Ben-Dror, J.; Shalamov, M.; Sonnenblick, A. The History of Early Breast Cancer Treatment. *Genes* **2022**, *13*, 960. [[CrossRef](#)]
16. Van den Ende, N.S.; Nguyen, A.H.; Jager, A.; Kok, M.; Debets, R.; van Deurzen, C.H.M. Triple-Negative Breast Cancer and Predictive Markers of Response to Neoadjuvant Chemotherapy: A Systematic Review. *Int. J. Mol. Sci.* **2023**, *24*, 2969. [[CrossRef](#)] [[PubMed](#)]
17. Lu, B.; Natarajan, E.; Raghavendran, H.R.B.; Markandan, U.D. Molecular Classification, Treatment, and Genetic Biomarkers in Triple-Negative Breast Cancer: A Review. *Technol. Cancer Res. Treat.* **2023**, *22*, 15330338221145246. [[CrossRef](#)]
18. Wang, Z.; Jiang, Q.; Dong, C. Metabolic reprogramming in triple-negative breast cancer. *Cancer Biol. Med.* **2020**, *17*, 44–59. [[CrossRef](#)] [[PubMed](#)]
19. Kim, C.; Gao, R.; Sei, E.; Brandt, R.; Hartman, J.; Hatschek, T.; Crosetto, N.; Foukakis, T.; Navin, N.E. Chemoresistance Evolution in Triple-Negative Breast Cancer Delineated by Single-Cell Sequencing. *Cell* **2018**, *173*, 879–893.e13. [[CrossRef](#)]
20. Manrique-Moreno, M.; Santa-González, G.A.; Gallego, V. Bioactive cationic peptides as potential agents for breast cancer treatment. *Biosci. Rep.* **2021**, *41*, BSR20211218C. [[CrossRef](#)]
21. Klaiss-Luna, M.C.; Giraldo-Lorza, J.M.; Jemioła-Rzemińska, M.; Strzałka, K.; Manrique-Moreno, M. Biophysical Insights into the Antitumoral Activity of Crotalidicin against Breast Cancer Model Membranes. *Int. J. Mol. Sci.* **2023**, *24*, 16226. [[CrossRef](#)]
22. Falcao, C.B.; de La Torre, B.G.; Pérez-Peinado, C.; Barron, A.E.; Andreu, D.; Rádis-Baptista, G. Viperidicins: A novel family of cathelicidin-related peptides from the venom gland of South American pit vipers. *Amino Acids* **2014**, *46*, 2561–2571. [[CrossRef](#)]
23. Falcao, C.B.; Radis-Baptista, G. Crotamine and crotalidicin, membrane active peptides from *Crotalus durissus terrificus* rattlesnake venom, and their structurally-minimized fragments for applications in medicine and biotechnology. *Peptides* **2020**, *126*, 170234. [[CrossRef](#)]
24. Falcao, C.B.; Pérez-Peinado, C.; de la Torre, B.G.; Mayol, X.; Zamora-Carreras, H.; Jiménez, M.Á.; Rádis-Baptista, G.; Andreu, D. Structural Dissection of Crotalidicin, a Rattlesnake Venom Cathelicidin, Retrieves a Fragment with Antimicrobial and Antitumor Activity. *J. Med. Chem.* **2015**, *58*, 8553–8563. [[CrossRef](#)]
25. Trinidad-Calderón, P.A.; Varela-Chinchilla, C.D.; García-Lara, S. Natural Peptides Inducing Cancer Cell Death: Mechanisms and Properties of Specific Candidates for Cancer Therapeutics. *Molecules* **2021**, *26*, 7453. [[CrossRef](#)] [[PubMed](#)]
26. Tornesello, A.L.; Borrelli, A.; Buonaguro, L.; Buonaguro, F.M.; Tornesello, M.L. Antimicrobial Peptides as Anticancer Agents: Functional Properties and Biological Activities. *Molecules* **2020**, *25*, 2850. [[CrossRef](#)]
27. Lin, T.-Y.; Weibel, D.B. Organization and function of anionic phospholipids in bacteria. *Appl. Microbiol. Biotechnol.* **2016**, *100*, 4255–4267. [[CrossRef](#)]
28. Pérez-Peinado, C.; Dias, S.A.; Domingues, M.M.; Benfield, A.H.; Freire, J.M.; Rádis-Baptista, G.; Gaspar, D.; Castanho, M.A.R.B.; Craik, D.J.; Henriques, S.T.; et al. Mechanisms of bacterial membrane permeabilization by crotalidicin (Ctn) and its fragment Ctn(15–34), antimicrobial peptides from rattlesnake venom. *J. Biol. Chem.* **2018**, *293*, 1536–1549. [[CrossRef](#)]
29. Pérez-Peinado, C.; Valle, J.; Freire, J.M.; Andreu, D. Tumor Cell Attack by Crotalidicin (Ctn) and Its Fragment Ctn [15–34]: Insights into Their Dual Membranolytic and Intracellular Targeting Mechanism. *ACS Chem. Biol.* **2020**, *15*, 2945–2957. [[CrossRef](#)]
30. Carrera-Aubersart, A.; Defaus, S.; Pérez-Peinado, C.; Sandín, D.; Torrent, M.; Jiménez, M.Á.; Andreu, D. Examining Topoisomers of a Snake-Venom-Derived Peptide for Improved Antimicrobial and Antitumoral Properties. *Biomedicines* **2022**, *10*, 2110. [[CrossRef](#)] [[PubMed](#)]
31. Gallego-Londoño, V.; Santa-González, G.A.; Giraldo-Lorza, J.M.; Rojas, M.; Wisman, G.B.A.; de Jong, S.; Manrique-Moreno, M. Crotalidicin and NA-CATH-ATRA-1-ATRA-1 peptide-induced membrane disruption in human breast cancer cells. *Biochim. et Biophys. Acta Biomembr.* **2025**, *1867*, 184429. [[CrossRef](#)] [[PubMed](#)]
32. Mandapati, A.; Lukong, K.E. Triple negative breast cancer: Approved treatment options and their mechanisms of action. *J. Cancer Res. Clin. Oncol.* **2022**, *149*, 3701–3719. [[CrossRef](#)]
33. Burridge, P.W.; Li, Y.F.; Matsa, E.; Wu, H.; Ong, S.-G.; Sharma, A.; Holmström, A.; Chang, A.C.; Coronado, M.J.; Ebert, A.D.; et al. Human induced pluripotent stem cell-derived cardiomyocytes recapitulate the predilection of breast cancer patients to doxorubicin-induced cardiotoxicity. *Nat. Med.* **2016**, *22*, 547–556. [[CrossRef](#)]
34. de Barros, E.; Gonçalves, R.M.; Cardoso, M.H.; Santos, N.C.; Franco, O.L.; Cândido, E.S. Snake Venom Cathelicidins as Natural Antimicrobial Peptides. *Front. Pharmacol.* **2019**, *10*, 1415. [[CrossRef](#)] [[PubMed](#)]
35. Camilio, K.A.; Wang, M.-Y.; Mauseth, B.; Waagene, S.; Kvalheim, G.; Rekdal, Ø.; Sveinbjørnsson, B.; Mælandsmo, G.M. Combining the oncolytic peptide LTX-315 with doxorubicin demonstrates therapeutic potential in a triple-negative breast cancer model. *Breast Cancer Res.* **2019**, *21*, 9. [[CrossRef](#)]

36. Vale, N.; Ribeiro, E.; Cruz, I.; Stulberg, V.; Kokschi, B.; Costa, B. New Perspective for Using Antimicrobial and Cell-Penetrating Peptides to Increase Efficacy of Antineoplastic 5-FU in Cancer Cells. *J. Funct. Biomater.* **2023**, *14*, 565. [[CrossRef](#)]
37. Yamazaki, T.; Pitt, J.M.; Vétizou, M.; Marabelle, A.; Flores, C.; Rekdal, Ø.; Kroemer, G.; Zitvogel, L. The oncolytic peptide LTX-315 overcomes resistance of cancers to immunotherapy with CTLA4 checkpoint blockade. *Cell Death Differ.* **2016**, *23*, 1004–1015. [[CrossRef](#)] [[PubMed](#)]
38. Raileanu, M.; Popescu, A.; Bacalum, M. Antimicrobial Peptides as New Combination Agents in Cancer Therapeutics: A Promising Protocol against HT-29 Tumoral Spheroids. *Int. J. Mol. Sci.* **2020**, *21*, 6964. [[CrossRef](#)] [[PubMed](#)]

**Disclaimer/Publisher's Note:** The statements, opinions and data contained in all publications are solely those of the individual author(s) and contributor(s) and not of MDPI and/or the editor(s). MDPI and/or the editor(s) disclaim responsibility for any injury to people or property resulting from any ideas, methods, instructions or products referred to in the content.